PULSE LENGTH ASSESSMENT OF COMPACT IGNITION TOKAMAK DESIGNS

PLASMA ENGINEERING

KEYWORDS: *tokamak, ignition, burn dynamics*

DAREN P. STOTLER and NEIL POMPHREY
Princeton University, Princeton Plasma Physics Laboratory
Princeton, New Jersey 08543

Received May 18, 1989
Accepted for Publication November 13, 1989

A time-dependent zero-dimensional code has been developed to assess the pulse length and auxiliary heating requirements of Compact Ignition Tokamak (CIT) designs. By taking a global approach to the calculation, parametric studies can be easily performed. The accuracy of the procedure is tested by comparison with the Tokamak Simulation Code, which uses theory-based thermal diffusivities. A series of runs is carried out at various levels of energy confinement for each of three possible CIT configurations. It is found that for cases of interest ignition or an energy multiplication factor $Q \gtrsim 7$ can be attained within the first half of the planned 5-s flattop with 10 to 40 MW of auxiliary heating. These results are supported by analytic calculations.

I. INTRODUCTION

Present designs of the Compact Ignition Tokamak[1] (CIT) are limited to a current flattop time of 5 s due to resistive heating of the toroidal field coils and other factors. Some of this 5 s is needed to complete the plasma heating process begun during the current ramp phase. The rest of the flattop time is then available for studying the physics of an ignited plasma. In this paper, we provide an estimate of the length of this period for three possible CIT configurations.

The time required to heat the plasma to ignition temperatures is directly related to the amount of auxiliary power available; thus, we can view this study as yielding the level of auxiliary heating needed to obtain a certain heating time.

Previous work along these lines employed complicated (and time-consuming) $1\frac{1}{2}$-dimensional transport simulations.[2,3] Since reliable transport models for this task do not exist in fully validated form, it is not clear that the extra effort required to proceed with these simulations would be worthwhile. Instead, we employ a code designed to follow the time evolution of the volume-integrated plasma energy. This approach results in a significant decrease in the time needed to analyze a particular discharge scenario. Hence, a number of studies spanning the envisioned parameter space can easily be carried out.

As has been pointed out elsewhere (see Ref. 4 and references therein, for example), the level of energy confinement in CIT is the most uncertain element in this type of calculation. If the thermal insulation is below a certain amount, it is difficult to attain values of the energy multiplication factor Q much in excess of unity without extraordinary auxiliary heating power (say, >40 MW). On the other hand, if the energy confinement is above some larger value, CIT should ignite readily with little or no auxiliary power input. The questions we wish to answer are relevant only in a band of energy confinement between these two extremes. In this range, we find for each CIT design that $Q \gtrsim 7$ or ignited operation can be achieved within the first half of the flattop for 10 to 40 MW of auxiliary power.

Several aspects of this problem are amenable to analytic solution. We present two simple models that show qualitatively how the time needed to heat the plasma depends on the auxiliary power available, the minimum auxiliary power required, and the plasma density. We then consider the consequences of using an energy confinement formula that depends on the input power rather than the plasma energy, as is assumed for the bulk of this work.

In Sec. II, we describe our global, time-dependent code and present a comparison with a sophisticated transport code. Section III contains the results of a

parametric study for three different CIT designs. The analytic calculations are presented in Sec. IV. Finally, we provide a summary in Sec. V.

II. TIME-DEPENDENT GLOBAL CODE

A number of global power balance codes have been developed recently.[5-9] They typically solve an equation similar to

$$P_\alpha + P_{\rm OH} + P_{aux} = P_{con} + P_{rad} \ . \tag{1}$$

The individual terms represent the volume-integrated contributions made to the total power balance by alpha, ohmic (OH), and auxiliary heating; thermal conduction and radiated losses are on the right side. We generalize this expression to include time dependence and helium ash accumulation:

$$\frac{dW_{tot}}{dt} = -P_{con} - P_{rad} + P_\alpha + P_{\rm OH} + P_{aux} \tag{2}$$

and

$$\frac{dN_{\rm He}}{dt} = \frac{P_\alpha}{E_\alpha} - \frac{N_{\rm He}}{\tau_{p,{\rm He}}} \ . \tag{3}$$

The various terms in Eq. (2) are described below. In Eq. (3), $N_{\rm He}$ is the number of helium ash particles, $E_\alpha = 3.5$ MeV is the alpha birth energy, and $\tau_{p,{\rm He}}$ is the (constant) helium ash particle confinement time. Equation (3) assumes that the slowing down of fast alpha particles takes place instantaneously. In reality, the alpha slowing down time in CIT is expected to be on the order of 100 ms.

Codes such as the one described here are zero-dimensional in that the plasma profiles are all specified on input. We use the following for density, temperature, and plasma current density:

$$x = x_0(1 - r^2/a^2)^{\alpha_x} \ , \tag{4}$$

where x is replaced by n, T, and J, respectively, and a is the plasma minor radius. Then, the alpha power is computed using

$$P_\alpha = E_\alpha 4\pi^2 R\kappa \int_0^a r\,dr\, n_{\rm D} n_{\rm T} \overline{\sigma v}_{\rm DT} \ , \tag{5}$$

where R is the plasma major radius and κ is the plasma elongation. The reactivity $\overline{\sigma v}_{\rm DT}$ is calculated with a formula obtained by Hively[10] in order to ensure correct results in all temperature regimes. Consequently, this integral must be computed numerically for each value of the density-weighted, volume-averaged temperature, $\langle T\rangle \equiv \langle n_e T\rangle / \langle n_e\rangle$.

The OH power is (all powers are in watts)

$$P_{\rm OH} = \frac{4.17 \times 10^3 Z_{eff} \ln\Lambda \gamma_{NC} T_0^{-3/2} V}{1 + 2\alpha_J - \frac{3}{2}\alpha_T} \times \left\{ \frac{B_T[1 + \kappa^2(1 + 2\delta^2 - 1.2\delta^3)]}{2\kappa R q_0} \right\}^2 \ , \tag{6}$$

where

Z_{eff} = effective charge

$\ln\Lambda$ = coulomb logarithm

γ_{NC} = neoclassical resistivity enhancement factor (constant, taken to be 2.5)

T_0 = central electron (and ion) temperature (keV)

B_T = toroidal magnetic field (T)

δ = triangularity

V = plasma volume (m^3)

and R and a are in metres. This expression for $P_{\rm OH}$ is essentially the same as that used by Uckan.[9]

We assume that the safety factor on axis q_0 is unity and compute $\alpha_J = q_{cyl}/q_0 - 1$. For the equivalent cylindrical safety factor, we take

$$q_{cyl} = \frac{5a^2 B_T}{RI_p} \frac{[1 + \kappa^2(1 + 2\delta^2 - 1.2\delta^3)]}{2} \ , \tag{7}$$

where I_p is the plasma current in mega-amperes. These units are used throughout this paper unless otherwise specified.

Only bremsstrahlung radiation is included[9] in P_{rad}:

$$P_{rad} = 5.31 \times 10^{-37} \frac{n_{e0}^2 T_0^{1/2} Z_{eff} V}{\left(1 + 2\alpha_n + \frac{1}{2}\alpha_T\right)} \ , \tag{8}$$

where n_{e0} is the central electron density.

Finally, the conducted losses are written as

$$P_{con} = \frac{W_{tot}}{\tau_E} = \frac{2.40 \times 10^{-16}(\langle n_e T\rangle + \langle n_i T\rangle)V}{\tau_E} \ . \tag{9}$$

The time dependence of P_{aux}, Z_{eff}, I_p, B_T, $\langle n_e\rangle$, and the plasma boundary shape are specified on input. We assume that there is one impurity of charge Z in addition to the helium ash. From the electron density, Z_{eff}, Z, and the helium ash density, we can compute the amount of hydrogen in the plasma, taken to be 50% deuterium and 50% tritium. Constant values of α_n and α_T are prescribed as well. Then, given initial conditions for W_{tot} and $N_{\rm He}$, Eqs. (2) and (3) can be integrated using standard techniques.

To estimate the accuracy of this procedure, we compare a simulation of CIT produced by the Tokamak Simulation Code[11] (TSC) with results from our code. The TSC is being used to evaluate the magnetics

design for CIT. In addition to the free-boundary equilibrium calculations required for this task, it carries out a complete time-dependent, $1\frac{1}{2}$-dimensional transport calculation.

The specific TSC simulation with which we compare is designated as F11D1. It is similar to the one described in detail in Ref. 12. We need to make two minor modifications to our zero-dimensional code to match features present in F11D1. First, a global calculation of the cyclotron radiation is included in P_{rad}. The TSC runs that are more recent than F11D1 employ a revised formulation of the cyclotron radiation. In these runs, cyclotron radiation losses are negligible for typical CIT parameters (see also Ref. 13); hence, we do not include them in the runs described in Sec. III. The second modification required is the installation of a feedback loop to adjust P_{aux} to maintain a total input power $P_\alpha + P_{aux} + P_{OH} \leq 110$ MW. This technique is not used in Sec. III.

From the TSC output, we take the field and shape ramps, shown in Fig. 1. The auxiliary power programming is included in Fig. 2; 15 MW of auxiliary power is input at $t = 4.5$ s, and another 15 MW is added at $t = 6$ s. The falloff of P_{aux} for $t > 7.5$ s is the result of the feedback loop explained above. The volume-averaged electron density is brought up linearly in time from $\langle n_e \rangle = 0$ at $t = 0$ to $\langle n_e \rangle = 3.1 \times 10^{20}$ m^{-3} at $t = 7.5$ s and held constant thereafter. The density and temperature profiles TSC obtains do not vary greatly during the simulation. We choose our profile peaking factors using

$$\frac{n_0}{\langle n \rangle} = 1 + \alpha_n$$

and

$$\frac{T_0}{\langle T \rangle} = \frac{(1 + \alpha_n + \alpha_T)}{(1 + \alpha_n)} ,$$

arriving at $\alpha_n = 0.58$ and $\alpha_T = 1.53$. As in TSC, we employ $Z_{eff} = 1.5$, $Z = 8$, and $\tau_{p,He} = 1$ s. This last choice is made so that the helium ash confinement time is the same order of magnitude as τ_E. We do not vary $\tau_{p,He}$ in Sec. III since the effects of hydrogenic depletion by ash accumulation have been discussed in detail elsewhere.[2,14,15]

It remains only to specify the form of τ_E. The TSC uses a generalization of the Tang transport model based on drift-wave turbulence.[16,17] The TSC expression for the thermal diffusivity $\chi(r)$ consists of two pieces, one for the ohmic regime and one for the auxiliary heated regime. The two are combined in a sum of squares sense. To get a corresponding global model, we write

$$\tau_E^{-2} = \tau_{NA}^{-2} + (c_\tau \tau_{aux})^{-2} , \qquad (10)$$

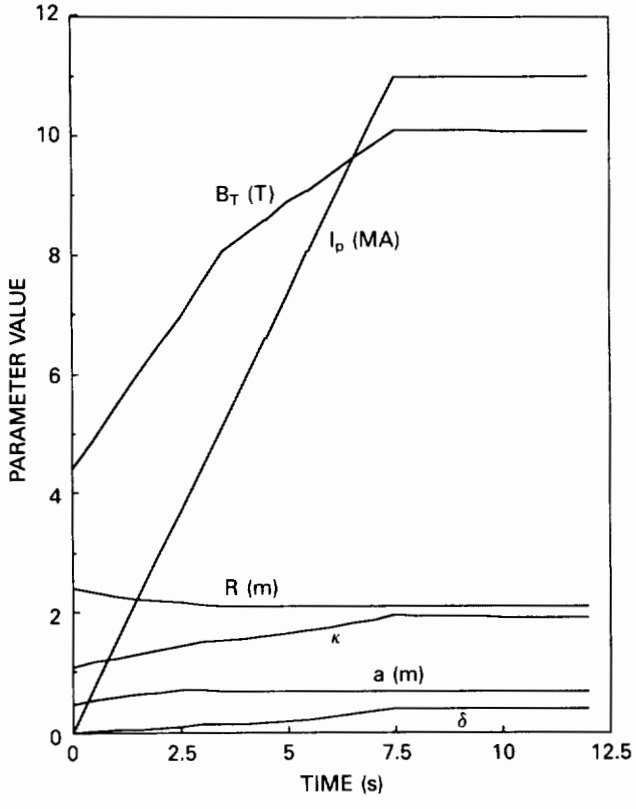

Fig. 1. Time dependence of various CIT parameters taken from TSC simulation F11D1.

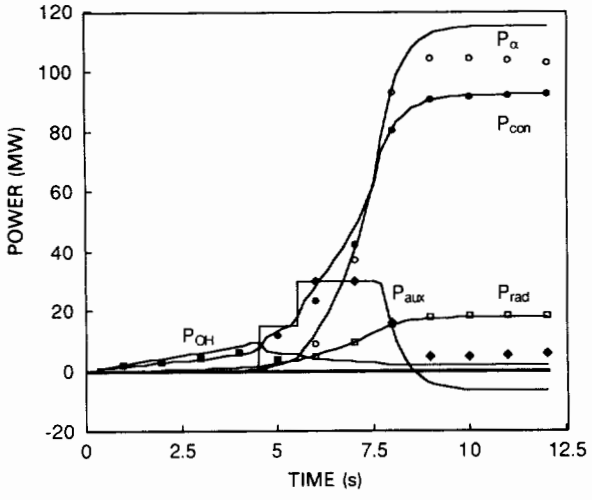

Fig. 2. Time dependence of the various terms in Eq. (2). The solid lines are the result of the zero-dimensional calculation. The markers indicate corresponding values taken from TSC output. Note that several of these points have been deleted for clarity. The solid squares represent P_{OH} from TSC; the diamonds are for P_{aux}.

where τ_{aux} is the scaling for auxiliary heated plasmas, and

$$\tau_{NA} = 7 \times 10^{-22} \bar{n}_e a R^2 q_{cyl} \quad (11)$$

is the neo-Alcator (ohmic) contribution, with $\bar{n}_e$ being the line-averaged electron density. The constant multiplier c_τ is specified on input.

We use the Kaye All-Complex L-mode scaling[4,18] for τ_{aux}:

$$\tau_{aux} = \tau_E^{KAC} = 0.0521 \bar{A}_i^{0.5} \kappa^{0.25} I_p^{0.85} \bar{n}_{e,19}^{0.1} B_T^{0.3} a^{0.3} R^{0.85} P_{in}^{-0.5} , \quad (12)$$

where

$\bar{A}_i$ = average ion mass (taken to be 2.5)

$\bar{n}_{e,19}$ = line-averaged electron density (10^{19} m^{-3})

$P_{in} = P_\alpha + P_{OH} + P_{aux} - P_{rad}$ = net input power (MW).

We intend for this P_{rad} to refer only to centrally peaked radiation mechanisms, such as bremsstrahlung, that affect the power balance in the center of the plasma. We evaluate τ_{NA} and τ_E^{KAC} at one point during the flattop of the TSC simulation and choose c_τ so that Eq. (10) yields the simulated value of τ_E. This procedure leads to $c_\tau = 1.9$.

The results of the comparison between the zero-dimensional model and TSC are shown in Fig. 2. We first note that the zero-dimensional estimate of P_{OH} is ~1 to 2 MW too large. Possible causes for this discrepancy are differences in current profile shape, flux surface shape, and neoclassical resistivity treatment. The total radiated power P_{rad} matches very well throughout. The alpha power P_α is ~10% larger in the zero-dimensional code than in TSC. This is due to differences in the density and temperature profile shapes, as well as differences in the plasma volume. The conducted powers agree by virtue of the feedback loop on P_{aux} and the choice of c_τ.

The error in the power balance brought on by the difference in P_α is absorbed by P_{aux} via the feedback loop. In particular, note that $P_{aux} < 0$ in the zero-dimensional code. From the point of view of Eq. (2), there is nothing peculiar about this. When it happens, P_{aux} makes a negative contribution to the P_{in} used in Eq. (12), but its effect on the outcome here is small since $|P_{aux}| \ll P_{in}$.

While permitting $P_{aux} < 0$ is physically unrealistic, it does allow us a clear comparison of the two simulations. In particular, we conclude that our error is ~10 MW out of 110 MW total input power, or ~10%.

III. PARAMETRIC STUDY FOR CIT

We examine three proposed magnetic configurations for CIT:

1. $I_p = 9$ MA, $B_T = 8.2$ T—present CIT design with existing Tokamak Fusion Test Reactor power supplies
2. $I_p = 11$ MA, $B_T = 10$ T—present CIT design with upgraded power supplies
3. $I_p = 13$ MA, $B_T = 11.8$ T—possible enhanced design using a bucked coil design.

For all three designs, $R = 2.1$ m, $a = 0.65$ m, $\kappa = 2$, and $\delta = 0.4$. The magnetic fields have been chosen in cases 1 and 3 to yield the same value of q_{cyl} as in case 2: $q_{cyl} = 2.73$. We take the field and shape ramps for the 11-MA device from TSC run F11D1 (Fig. 1) and rescale the I_p and B_T programming for the other two cases.

The input parameters are as in Sec. II, with the following exceptions. The energy confinement time is written as

$$\tau_E = min[\tau_{NA}, c_\tau^2 \tau_E^{KAC}(W_{tot})] . \quad (13)$$

This expression is more appropriate since the data base from which τ_E^{KAC} is derived contains numerous low-power discharges.[19] The neo-Alcator contribution is included only to provide a reasonable behavior when $\langle n_e \rangle$ and $\langle T \rangle \to 0$. We have also rewritten the scaling in terms of the plasma energy instead of the input power. The means of doing this and its consequences are described in Sec. IV.B. The multiplier c_τ is squared in Eq. (13) as a result of the conversion procedure. It is still a *linear* multiplier on the power form of τ_E^{KAC}. In the results described below, c_τ is varied systematically.

Note that when the confinement in H-mode discharges is compared with that of L-mode scalings (e.g., $\tau_{E,H} \sim 2\tau_{E,L}$, as in Ref. 18), the power form of τ_E is usually used for the latter. It is for this reason that we take c_τ (and not c_τ^2) to be the fundamental multiplier on τ_E.

Another difference from Sec. II is that instead of assuming a step function increase, we ramp the auxiliary heating power linearly with time between $t = 4.5$ and 5.5 s. This is a more plausible representation of the increase in heating efficiency expected to take place as the ion cyclotron frequency resonance layer moves toward the plasma center during the magnetic field ramp. The auxiliary power is held constant thereafter.

We can vary the amount and the time of heating. For ignited cases, we remove the auxiliary heating once the discharge has reached the point of ignition. For slightly subignited cases, we suddenly reduce P_{aux} at some point during the current flattop in order to maintain the fusion power and total β at reasonable levels. We do not address means of similarly controlling ignited discharges. Since the alpha power dominates the input power in these subignited cases ($P_{aux} \ll P_\alpha$; i.e., $Q \gg 1$), studying them should provide as much insight into the physics of alpha-particle heating as would

studying ignited scenarios. In all other instances, the auxiliary heating remains at full power until the end of the run.

The performance of CIT is very sensitive to the value of c_τ. Given that it would be unrealistic to plan for much more than 40 MW of auxiliary power on CIT, we are restricted in how small c_τ can be in order to attain $Q > 5$ operation. Below this level of confinement, the most desirable operating point (with $P_{aux} \leq 40$ MW) is at a sufficiently low temperature that the time needed to heat the plasma is short. Likewise, above some larger value of c_τ, ohmic ignition is possible. In this case, the time required to reach ignition, perhaps with a small amount of auxiliary power, is short enough that it is, again, pointless to do the calculation. We examine three values of c_τ lying between these two extremes.

For each c_τ, we consider separately two values of P_{aux} ($10 \leq P_{aux} \leq 40$ MW) in order to give some idea of the range of modes of operation possible at that level of confinement. We pick the flattop $\langle n_e \rangle$ to yield the highest Q or quickest ignition at each auxiliary power level. We require that the line-averaged density be less than[20]

$$\bar{n}_{e,max} = \frac{2B_T}{Rq_e} 10^{20} \text{ m}^{-3} , \quad (14)$$

where $q_e = 5a^2\kappa B_T/RI_p$ is the engineering q value. As in the TSC comparison, the density is ramped linearly from zero between $t = 0$ and 7.5 s.

For each of the three CIT configurations, there are three c_τ values, each run with two levels of auxiliary heating. This makes a total of 18 simulations. The results are summarized in Table I. As is demonstrated in Sec. IV.A, a finite Q state is approached logarithmically in time (ignoring helium ash buildup), and much of the flattop is spent attaining the last few increments in Q. So, we take the 90% Q_{max} point as characteristic of the time required to heat the plasma in these cases. The $Q \gg 1$ simulations are distinguished by the

TABLE I

Parameters for the 18 Time-Dependent Simulations

	P_{aux} (MW)	$\langle n_{e,20} \rangle$ (10^{20} m^{-3})	$P_{\alpha,max}$	Q_{max}	Heating Off Time	$t(P_{\alpha,max})$ or $t(0.9Q_{max})$
$I_p = 9$ MA						
$c_\tau = 1.6$	20	2.2	31	7.7	---	8.7
	40	3.2	69	8.6	---	8.3
$c_\tau = 1.9$	10	2.6	44	22	---	11.3
	20	3.5	82	41 (at 10 MW)	---	9.6
$c_\tau = 2.2$	10	3.5	56	∞[a]	9.6	12.0
	20	3.5	171	∞	7.5	11.7
$I_p = 11$ MA						
$c_\tau = 1.3$	20	2.2	36	8.9	---	8.5
	40	3.3	80	10	---	8.3
$c_\tau = 1.6$	20	3.8	106	266 (at 2 MW)	---	8.7
	30	4.3	120	∞	7.8	8.5
$c_\tau = 1.9$	10	4.3	135	∞	8.7	12.0
	20	4.3	333	∞	7.5	9.3
$I_p = 13$ MA						
$c_\tau = 1.0$	20	2.1	27	6.7	---	8.3
	40	3.0	56	7.0	---	8.1
$c_\tau = 1.3$	10	3.0	54	68 (at 4 MW)	---	10.9
	30	4.6	151	∞	8.2	8.3
$c_\tau = 1.6$	10	5.1	241	∞	8.9	12.0
	20	5.1	492	∞	7.5	9.3

[a]Ignited cases are indicated by $Q_{max} = \infty$.

additional entry "at x MW" in the Q_{max} column. For these runs, P_{aux} is reduced to x MW at some point prior to $t(0.9Q_{max})$ and held there for the remainder of the discharge.

As examples, we present in Figs. 3, 4, and 5 results for the 11-MA configuration with $c_\tau = 1.6$. In Fig. 3, the contours of constant auxiliary power required to maintain steady state at a given $\langle n_e \rangle$ and $\langle T \rangle$ are plotted (see, for example, Refs. 6 and 9). This type of diagram is referred to as a Plasma OPeration CONtour or POPCON plot.[21] The density and beta limits [β_{max} (%) = $3I_p/aB_T$] are also indicated. Figure 3 is constructed using the flattop parameters (i.e., $t \geq 7.5$ s) and does not assume any helium ash buildup. For this c_τ, we examine P_{aux} = 20 and 30 MW. The densities for these cases are $\langle n_{e,20} \rangle = 3.8$ and 4.3, respectively.

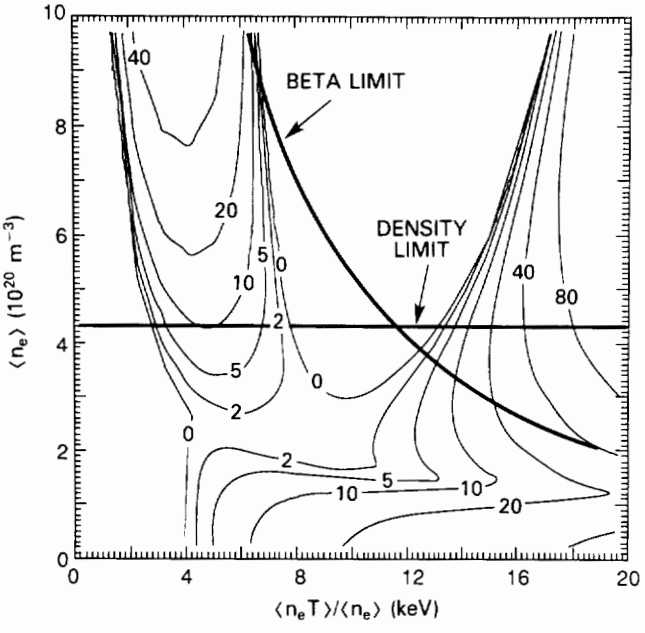

Fig. 3. Contours of constant auxiliary power in megawatts in $\langle n_e \rangle$ and $\langle T \rangle$ space for the 11-MA design with $c_\tau = 1.6$. The density and beta limits are indicated.

The time dependence of the terms in Eq. (2) for the 20-MW case is shown in Fig. 4. According to Fig. 3, this case should be ignited. But there is sufficient helium ash buildup ($n_\alpha/n_e = 0.014$ at $t = 12$ s) during the discharge to close the relatively small ignition window present at this density. However, $Q \gg 1$ operation is possible. So, when $\langle T \rangle$ reaches ~9 keV (t = 8.6 s), we reduce P_{aux} to 2 MW. At the end of the run, $\langle T \rangle = 9.7$ keV.

By raising the density to the maximum allowed, $\langle n_e \rangle = 4.3 \times 10^{20}$ m^{-3}, we can achieve ignition at this value of c_τ (Fig. 5). To overcome the increased thermal inertia without having to heat through most of the flattop, however, we need to raise P_{aux} to 30 MW. We turn off the auxiliary heating when $\langle T \rangle \simeq 9$ keV. Again, the helium ash buildup ends the ignition soon after it starts. By the end of the calculation, $\langle T \rangle$ drops to 8.5 keV.

With the freedom to vary P_{aux} between 10 and 40 MW and to choose any operating density below the prescribed density limit, we have been able to reach ignition (in the higher confinement cases) or at least $Q \gtrsim 7$ within the first half of the flattop ($t < 10$ s) in most of the cases reported in Table I. Greater restrictions on the auxiliary power available, the density, the level of confinement, or on the fusion power could lead to scenarios in which the full flattop time is needed to reach the desired operating point.

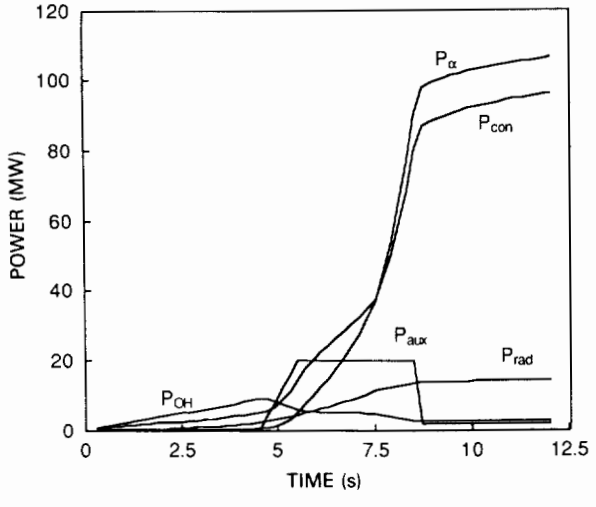

Fig. 4. Time dependence of the various terms in Eq. (2) for the 11-MA configuration of CIT with $c_\tau = 1.6$ and $\langle n_e \rangle = 3.8 \times 10^{20}$ m^{-3}.

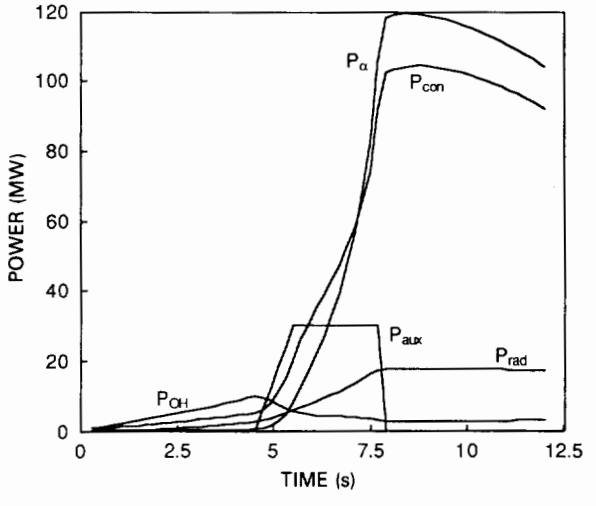

Fig. 5. Time dependence of the various terms in Eq. (2) for the 11-MA configuration of CIT with $c_\tau = 1.6$ and $\langle n_e \rangle = 4.3 \times 10^{20}$ m^{-3}.

IV. ANALYTIC CALCULATIONS

Several aspects of this problem can be addressed analytically. Waltz et al.[5] provide a general expression for the power P_s required to maintain steady state at the saddle point; this is the absolute minimum power required for ignition.[6,9,21] It is easy to show that $P_s \lesssim 10$ MW in CIT for the Kaye All-Complex scaling when the confinement is good enough to allow ignition below the density limit,[22] Eq. (14). The same is true, to within a factor of order unity, for other confinement expressions given the same limiting density (see the expression for Q at the saddle point in Ref. 5). The Waltz et al. expressions also yield for the Kaye All-Complex scaling a density at the saddle point $\langle n_e \rangle \propto c_\tau^{-10}$. This large exponent is the result of the weak density dependence of Eq. (12) and is connected to the sensitivity of CIT performance to c_τ noted in Sec. III.

We develop two simple models to describe the time required to heat the plasma in terms of quantities found on a POPCON plot. We then demonstrate that the use of a power-dependent confinement scaling instead of one written in terms of the plasma energy can almost double the required heating time.

IV.A. Time Required to Heat the Plasma

It is difficult to integrate Eq. (2) analytically in general. Some of the problem terms can be neglected, but the results still tend to be too complicated to provide insight. What we seek to do here instead is to model the most important structure displayed in POPCON plots (e.g., Fig. 3) in such a way that Eq. (2) can be integrated exactly, yielding $W_{tot}(t)$ or at least $t(W_{tot})$.

We first consider cases in which ignition is possible within the prescribed density and beta limits, Fig. 3 for example. The precise question we seek to answer is: How long does it take to heat from the ohmic equilibrium contour to the ignited equilibrium contour? This, of course, depends on the path in $\langle n_e \rangle$ and $\langle T \rangle$ space.

We assume for the moment that all parameters except for $\langle n_e \rangle$ and $\langle T \rangle$ are fixed during this process. Then, all of the variations in dW_{tot}/dt can be deduced from a POPCON diagram, i.e., a contour plot of

$$P_{pb}(\langle n_e \rangle, \langle T \rangle) \equiv \frac{W_{tot}}{\tau_E} + P_{rad} - P_\alpha - P_{\mathrm{OH}} \ . \quad (15)$$

The subscript pb refers to power balance. In an ignited case, P_{pb} goes through a maximum along a constant density path between the ohmic and ignited equilibrium contours. We can model this behavior at least near the maximum with a parabola:

$$P_{pb} = a\langle T \rangle^2 + b\langle T \rangle + c \ . \quad (16)$$

By specifying P_{pb} at two points (for example, one on each of the ohmic and ignited equilibrium contours) and the maximum value P_m of P_{pb} along the path, the coefficients a, b, and c can be determined. The range in $\langle T \rangle$ over which Eq. (16) is accurate is determined by the size of $\partial^3 P_{pb}/\partial \langle T \rangle^3$. Since we are only looking for a qualitative answer, we can neglect such higher order derivatives and take Eq. (16) to be valid at least between the points at which we specify P_{pb}.

It is more convenient to express Eq. (16) in terms of W_{tot}; we assume that

$$P_{pb} = aW_{tot}^2 + bW_{tot} + c \ . \quad (17)$$

This allows for cases in which the density or even some of the other parameters in the calculation vary in time, during the current ramp phase of CIT for example. If most of the heating is done during the flattop, we can still use a POPCON to obtain an estimate of P_m.

We now assume that we know $P_{pb}(W_0) = P_0$ and $P_{pb}(W_1 > W_0) = P_1$ and the maximum value of P_{pb} between W_0 and W_1, P_m. We allow P_0 and P_1 to be nonzero to account for cases in which ohmic ignition is possible. If the system has energy W_i at time t_i, and a constant auxiliary power P_{aux} is applied until the energy reaches W_f at time t_f, we can integrate Eq. (2) using Eqs. (15) and (17) to obtain

$$t_f - t_i = \frac{W_1 - W_0}{(\Delta P_a)^{1/2}[(\Delta P_0)^{1/2} + (\Delta P_1)^{1/2}]} \times \left[\tan^{-1}\left\{ \left[\left(\frac{\Delta P_0}{\Delta P_a}\right)^{1/2} + \left(\frac{\Delta P_1}{\Delta P_a}\right)^{1/2} \right] \times \left(\frac{W - \overline{W}}{W_1 - W_0}\right) + \frac{1}{2}\left[\left(\frac{\Delta P_1}{\Delta P_a}\right)^{1/2} - \left(\frac{\Delta P_0}{\Delta P_a}\right)^{1/2} \right] \right\} \right]_{W_i}^{W_f} , \quad (18)$$

where

$$\overline{W} \equiv (W_0 + W_1)/2$$
$$\Delta P_0 \equiv P_m - P_0$$
$$\Delta P_1 \equiv P_m - P_1$$
$$\Delta P_a \equiv P_{aux} - P_m .$$

In the limit of $P_{aux} \gg P_m$, Eq. (18) becomes

$$t_f - t_i \simeq \frac{W_f - W_i}{P_{aux}} \ , \quad (19)$$

as expected.

If we take Eq. (17) to hold for all W_{tot}, as if P_α would continue to dominate P_{con} with increasing T, $W_{tot} \to \infty$ in a finite time. This defines a characteristic time to heat to ignition:

$$t_f - t_i \sim \frac{\pi}{2} \frac{W_1 - W_0}{(\Delta P_a)^{1/2}[(\Delta P_0)^{1/2} + (\Delta P_1)^{1/2}]} \ . \quad (20)$$

In this expression, ΔP_a represents the excess input power; ΔP_0 and ΔP_1 describe the steepness of $P_{pb}(W_{tot})$ and are thus directly related to the rate at which the thermal instability proceeds.

Typical numbers for an ignited CIT would be (as in Fig. 3) $W_f - W_i \sim W_1 - W_0 \sim 50$ MJ, $P_1 \simeq P_0 \simeq 0$, and $P_m \simeq 10$ MW. For convenience, we have set $W_i = W_0$ and $W_f = W_1$. With these values and $P_{aux} = 20$ MW, Eqs. (18) and (20) yield exactly the same result: $t_f - t_i = 4$ s.

For most ignited CIT cases, $P_m < 10$ MW, and we may even have $P_m \lesssim 0$ (ohmic ignition). In this case, Eq. (19) provides an approximate lower limit to the time required to heat the plasma: $t_f - t_i \simeq 2.5$ s.

Returning now to Table I, using $t_i \simeq 5$ s and setting t_f in the ignited cases equal to the heating off time, we see that the range $t_f - t_i = 2.5$ to 4 s also describes our numerical calculations fairly well.

We now consider cases with finite Q. In this instance, the path from ohmic equilibrium to the final state is one of monotonically increasing P_{pb}, as in the moderate-density, high-temperature region of Fig. 3. For small c_τ, the conducted losses dominate for all temperatures above ohmic equilibrium, provided $\langle n_e \rangle$ is not so large as to make radiation dominant. In the limit of $c_\tau \to 0$, $P_{pb} \propto \langle T \rangle^2$ (assuming $\tau_E \propto P_{in}^{-0.5}$). The finite Q cases examined in Table I have more moderate c_τ. For them, the alpha power effectively reduces the rate of rise of P_{pb} below $\langle T \rangle^2$.

We model these cases qualitatively by linearly interpolating between two points on the POPCON. We specify the plasma energy at ohmic equilibrium, $W_{\rm OH}$, and the energy attained in the limit $t \to \infty$ for a given P_{aux}, $W_{P_{aux}}$. Thus,

$$P_{pb}(W_{tot}) = \left(\frac{W_{tot} - W_{\rm OH}}{W_{P_{aux}} - W_{\rm OH}} \right) P_{aux} \ . \qquad (21)$$

Integration of Eq. (2) using Eqs. (15) and (21) with initial and final energies W_i and W_f, respectively, yields

$$t_f - t_i = \frac{W_{P_{aux}} - W_{\rm OH}}{P_{aux}} \ln \left(\frac{1 - W_i/W_{P_{aux}}}{1 - W_f/W_{P_{aux}}} \right) \ . \qquad (22)$$

Note that the time required to heat the plasma diverges logarithmically as W_f approaches $W_{P_{aux}}$.

To provide some typical values for these quantities, we give in Table II data from the $Q \sim 7$ to 10 runs of Sec. III. We evaluate t_i and $W_{\rm OH}$ at the earliest time for which $P_{aux} > P_{\rm OH}$. Since Q increases roughly like W_{tot}^2, we assume $W_f = 0.95 W_{P_{aux}}$ in Table II so that we can compare with the $t(0.9Q_{max})$ entry in Table I. This is meant only as a qualitative comparison since the above model is considerably simpler than the one used in the actual numerical calculations.

In Table II, we see that the time required to heat the plasma is ~2.5 to 3.5 s, as was the case for the ignited discharges. We reiterate that this is the result of judicious choices of $\langle n_e \rangle$ and P_{aux} and does not necessarily indicate any fundamental limitation. The effects of these choices are evident in each of Eqs. (18), (19), (20), and (22). The thermal inertia of the plasma increases linearly with $\langle n_e \rangle$, and the heating time decreases uniformly with P_{aux}. Between these two parameters, there is enough freedom to arrange for $t_f - t_i$ to fall within the range desired for CIT.

TABLE II

Time Required to Heat Plasma to 95% of $W_{P_{aux}}$ Evaluated Using Data from Table I and Eq. (22)

I_p	c_τ	P_{aux}	$W_{\rm OH}$	$W_{P_{aux}}$	$t(0.95W_{P_{aux}})$
9	1.6	20	5.5	30	8.3
9	1.6	40	6.2	46	7.5
11	1.3	20	6.4	33	8.5
11	1.3	40	9.2	48	7.6
13	1.0	20	8.6	28	7.7
13	1.0	40	9.4	41	7.1

IV.B. Energy Versus Power Form of τ_E

Theories of tokamak energy confinement generally express their results in terms of local plasma parameters, n_e and T. It is for this reason that we have been using the energy form of τ_E up to this point. On the other hand, experimental values of τ_E are most readily categorized by input power P_{in} and the line-averaged density since they can be obtained with relatively little data analysis. In steady state, the two forms of τ_E are related by

$$P_{in} = \frac{W_{tot}}{\tau_E} \ , \qquad (23)$$

This is equivalent to Eq. (1) when we interpret P_{in} as the net input power:

$$P_{in} = P_{\rm OH} + P_\alpha + P_{aux} - P_{rad} \ .$$

With

$$\tau_E(P_{in}) = f_\tau P_{in}^{-\gamma} \ , \qquad (24)$$

where f_τ contains all of the nonpower dependence (including the multiplier c_τ), this procedure yields

$$\tau_E(W_{tot}) = (f_\tau W_{tot}^{-\gamma})^{1/(1-\gamma)} \ . \qquad (25)$$

Since scaling expressions are based on data[18] for which $\dot{W}_{tot} \ll P_{in}$ (i.e., steady state), the energy and power forms fit the data base equally well. Hence, there are no empirical reasons to choose one over the other. When the plasma is not in steady state [Eq. (23) is not satisfied], the two forms of τ_E yield different

values of $\dot{W}_{tot}$ as obtained from Eq. (2). Thus, while a steady-state power balance calculation (e.g., a POPCON) is indifferent as to which representation is used, a time-dependent calculation [e.g., Eq. (2)] is not.

We can estimate the difference in the times to heat to ignition for the two forms of τ_E as follows. Define $\dot{W}_{tot}$ as the value of dW_{tot}/dt obtained with $\tau_E(P_{in})$, and $\dot{W}'_{tot}$ as that found with $\tau_E(W_{tot})$. We can then show

$$\frac{\tau_E(W_{tot})}{W_{tot}}\dot{W}_{tot} = 1 + \frac{\tau_E(W_{tot})}{W_{tot}}\dot{W}'_{tot} - \left[1 + \frac{\tau_E(W_{tot})}{W_{tot}}\dot{W}'_{tot}\right]^{\gamma} . \quad (26)$$

In the limit

$$\frac{\tau_E(W_{tot})}{W_{tot}}\dot{W}'_{tot} \ll 1$$

(the time rate of change of the plasma energy is much less than the conducted losses), we can expand the term in brackets to obtain

$$\dot{W}_{tot} \simeq \dot{W}'_{tot}(1-\gamma) . \quad (27)$$

In the opposite limit (valid when $P_{aux} \gg P_{con}$), $\dot{W}_{tot} \simeq \dot{W}'_{tot}$.

For the cases considered in Sec. III, the first limit is more appropriate. Noting that $\gamma = 0.5$ for the Kaye All-Complex scaling, we see that $\dot{W}_{tot}$ would be reduced by a factor of 2 if we were to use the power form of τ_E. In other words, it would take twice as long to increase W_{tot} by a specific amount.

Figures 6 and 7 show calculations identical to those given in Figs. 4 and 5, respectively, but with the power form of τ_E replacing the energy form. The heating off times have been altered to yield the same maximum P_α. Note that the total heating times required with the power form are less than double that needed with the energy form due to finite values of $[\tau_E(W_{tot})/W_{tot}]\dot{W}'_{tot}$.

In Sec. III, we were able to arrange the parameters of the various simulations so that the desired plasma operation point could be reached within the first half of the flattop. The above result then suggests that with the power form of τ_E, we could still achieve roughly the same end states under the assumptions of Sec. III by the end of the flattop period. By examining experimental data, it may be possible to demonstrate that one of these two ways of writing τ_E is more appropriate than the other.

V. SUMMARY

In summary, we have assessed the pulse length and auxiliary heating requirements for three possible CIT designs. To this end, a time-dependent zero-dimensional code has been developed. Our procedures have been checked by comparing them against a TSC simulation of CIT. In this comparison, we have found that the flattop power balance matches to within ~10 MW out of ~100 MW for each of the dominant terms.

The results of this paper are presented in Sec. III, where we have given parameters from several simulations of each suggested CIT magnetic configuration. For the lowest levels of confinement examined in each machine, $P_{aux} = 40$ MW is required to achieve

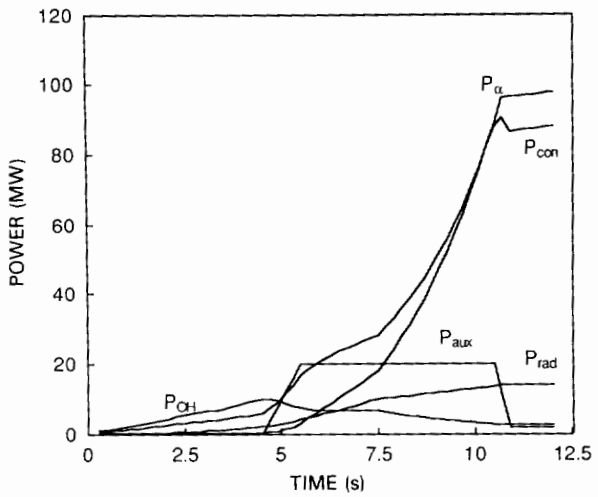

Fig. 6. Time dependence of the various terms in Eq. (2) for the 11-MA configuration of CIT with $c_\tau = 1.6$ (using the power-dependent form of τ_E) and $\langle n_e \rangle = 3.8 \times 10^{20}$ m^{-3}.

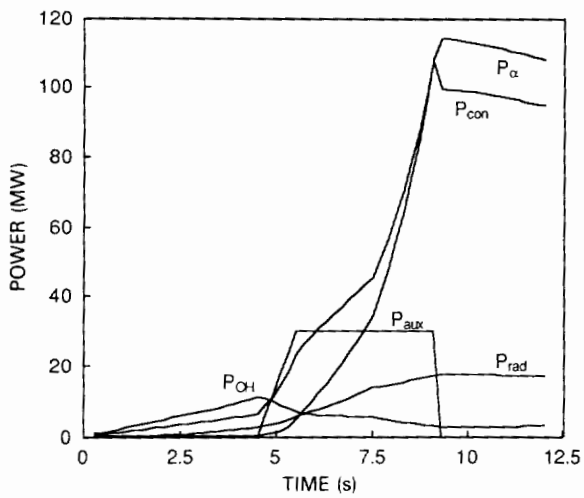

Fig. 7. Time dependence of the various terms in Eq. (2) for the 11-MA configuration of CIT with $c_\tau = 1.6$ (using the power-dependent form of τ_E) and $\langle n_e \rangle = 4.3 \times 10^{20}$ m^{-3}.

$P_\alpha \sim 60$ MW. While $P_{aux} = 20$ MW is sufficient to reach similar values of Q ($Q \gtrsim 7$), the resulting P_α is, of course, proportionately smaller. For the cases with better confinement, $Q \gg 1$ or ignited operation is obtained with $P_{aux} \leq 20$ MW. The freedom to adjust P_{aux} and the plasma density has allowed us to reach these final plasma operating states during the first half of the current flattop.

Two analytic calculations have been presented. We first described simple models for the time required to heat the plasma, one for ignited cases and one for finite Q operation. In both instances, application of the formulas to typical CIT scenarios yielded heating times of 2.5 to 4 s, in qualitative agreement with Sec. III.

We then considered the consequences of writing τ_E in terms of the input power rather than the plasma energy, as was done throughout the rest of the paper. We have found that with the former, the time required to heat the plasma through a given range of plasma energy is almost twice as long as for the latter. Since the simulations of Sec. III required less than ~4 s to heat to the desired operating point, we would still be able to reach roughly the same final states by the end of the flattop even if this more pessimistic scaling is the appropriate description of the plasma.

ACKNOWLEDGMENTS

The authors would like to acknowledge the numerous comments on this work provided by the CIT team. This work was supported by U.S. Department of Energy contract DE-AC02-76-CHO-3073.

REFERENCES

1. R. R. PARKER et al., "CIT Physics and Engineering Basis," *Proc. 12th Int. Conf. Plasma Physics and Controlled Nuclear Fusion*, Nice, France, October 12–19, 1988, paper IAEA-CN-50/G-II-1, p. 341, International Atomic Energy Agency (1989); see also J. A. SCHMIDT and H. P. FURTH, "Compact Ignition Tokamak Conceptual Design Report," A-860606-P-01, Princeton Plasma Physics Laboratory (June 1986).

2. D. P. STOTLER and G. BATEMAN, "Time-Dependent Simulations of a Compact Ignition Tokamak," *Fusion Technol.*, **15**, 12 (1989).

3. C. E. SINGER, L.-P. KU, and G. BATEMAN, "Plasma Transport in a Compact Ignition Tokamak," *Fusion Technol.*, **13**, 543 (1988).

4. D. P. STOTLER, R. J. GOLDSTON, and the CIT Team, "Ignition Probabilities for Compact Ignition Tokamak Designs," PPPL-2629, Princeton Plasma Physics Laboratory (1989).

5. R. E. WALTZ, R. R. DOMINGUEZ, and F. W. PERKINS, "Drift Wave Model Tokamak Ignition Projections with a Zero-Dimensional Transport Code," *Nucl. Fusion*, **29**, 351 (1989).

6. N. A. UCKAN and J. SHEFFIELD, "A Simple Procedure for Establishing Ignition Conditions in Tokamaks," *Tokamak Startup*, p. 45, H. KNOEPFEL, Ed., Plenum Press, New York (1986).

7. Y. C. SUN, D. E. POST, G. BATEMAN, and D. STOTLER, "The Performance of CIT and ITER Under Various Scaling Laws," *Bull. Am. Phys. Soc.*, **33**, 1971 (1988).

8. O. MITARAI, A. HIROSE, and H. M. SKARSGARD, "Generalized Ignition Contour Map and Scaling Law Requirement for Reaching Ignition in a Tokamak Reactor," *Nucl. Fusion*, **28**, 2141 (1988).

9. N. A. UCKAN, "Relative Merits of Size, Field, and Current on Ignited Tokamak Performance," *Fusion Technol.*, **14**, 299 (1988).

10. L. M. HIVELY, "Convenient Computational Forms for Maxwellian Reactivities," *Nucl. Fusion*, **17**, 873 (1977).

11. S. C. JARDIN, N. POMPHREY, and J. DE LUCIA, "Dynamic Modeling of Transport and Positional Control of Tokamaks," *J. Comput. Phys.*, **66**, 481 (1986).

12. N. POMPHREY, "The 11 MA Fiducial Discharge," AE-890417-PPL-04, Princeton Plasma Physics Laboratory (1989).

13. W. A. HOULBERG, "Synchrotron Radiation Losses in CIT," P-870615-PPL-01, Princeton Plasma Physics Laboratory (1987).

14. S. C. HU and G. H. MILEY, "Alpha Ash Effect and Control in TIBER-II," *Proc. 12th Symp. Fusion Engineering*, Monterey, California, October 12–16, 1987, p. 1461, Institute of Electrical and Electronics Engineers (1987).

15. M. H. REDI and S. A. COHEN, "Effects of Particle Transport on Sustained Ignition in the ITER Design," presented at Sherwood Theory Meeting, San Antonio, Texas, April 3–5, 1989, paper 2D31, Science Applications International Corporation (1989).

16. S. C. JARDIN, J. DE LUCIA, M. OKABAYASHI, N. POMPHREY, M. REUSCH, S. KAYE, and H. TAKAHASHI, "Post-Disruptive Plasma Loss in the Princeton Beta Experiment (PBX)," *Nucl. Fusion*, **27**, 569 (1987).

17. W. M. TANG, "Microinstability-Based Model for Anomalous Thermal Confinement in Tokamaks," *Nucl. Fusion*, **26**, 1605 (1986).

18. ITER Team, *ITER Concept Definition, Vol. 2*, International Atomic Energy Agency (1989); see also S. M. KAYE, C. W. BARNES, M. G. BELL, J. C. DE BOO,

M. GREENWALD, K. RIEDEL, D. SIGMAR, N. UCKAN, and R. WALTZ, "Status of Global Energy Confinement Studies," PPPL-2670, Princeton Plasma Physics Laboratory (Feb. 1990).

19. S. M. KAYE, Princeton Plasma Physics Laboratory, Private Communication (1989).

20. JET Team, "JET Latest Results and Future Prospects," *Proc. 12th Int. Conf. Plasma Physics and Controlled Nuclear Fusion*, Nice, France, October 12–19, 1988, paper IAEA-CN-50/A-I-3, p. 41, International Atomic Energy Agency (1989).

21. W. A. HOULBERG, S. E. ATTENBERGER, and L. M. HIVELY, "Contour Analysis of Fusion Reactor Plasma Performance," *Nucl. Fusion*, **22**, 935 (1982).

22. D. P. STOTLER and N. POMPHREY, "Pulse Length Assessment of Compact Ignition Tokamak Designs," PPPL-2630, Princeton Plasma Physics Laboratory (July 1989); see also D. P. STOTLER, N. POMPHREY, R. J. GOLDSTON, and M. G. BELL, "Pulse Length and Ignition Probability Studies for the Compact Ignition Tokamak," *Proc. Sherwood Theory Mtg.*, San Antonio, Texas, April 3–5, 1989, paper 3C32, Science Applications International Corporation (1989).